FLUX ANALYSIS OF DUST PARTICLES GENERATED BY SOLID ROCKET MOTOR RETRO-BURNS

S. Stabroth[1], M. Homeister, M. Oswald, C. Wiedemann, P. Vörsmann
Institute of Aerospace Systems, Technische Universität Braunschweig,
Hermann-Blenk-Str. 23, 38108 Braunschweig

H. Klinkrad
Space Debris Office, ESA/ESOC, Robert-Bosch-Str. 5, 64293 Darmstadt

OVERVIEW

The ESA space debris population model MASTER-2005 (Meteoroid and Space Debris Terrestrial Environment Reference) considers firings of solid rocket motors (SRM) as a debris source with the generation of slag and dust particles. The resulting object population contributes to the sub-millimetre size debris environment in Earth orbit. A comparison of the modelled debris flux with impact data from returned surfaces shows that the shape and quantity of the modelled SRM dust distribution matches that of recent Hubble Space Telescope (HST) solar array measurements very well. However, the absolute flux level for dust is under-predicted for some of the analysed Long Duration Exposure Facility (LDEF) surfaces. This points into the direction of some past firings which are not included in the current event database consisting of 1,076 orbital SRM burns. The most suitable candidates for these firings are retro-burns of return capsules. Objects released by those firings have highly eccentric orbits with perigees in the lower atmospheric regions. They produce no long-term effect on the debris environment. However, a large number of those firings during the on-orbit time frame of LDEF might lead to an increase of the dust population for some of the LDEF surfaces. In this paper, the influence of Russian SRM retro-burns on the debris environment is analysed.

1. INTRODUCTION

The MASTER model allows for a simulation of particle releases due to firings of solid rocket motors (SRM) in addition to other space debris sources. In the exhaust gas of typical SRM engines, a considerable amount of small aluminium oxide particles is included. Aluminium is used as an additive in the motor propellant in order to increase performance and to dampen burn instabilities. During the burn process most of this aluminium is transformed into aluminium oxide. A large number of micron-sized dust particles is generated continuously during a burn. At the end of a burn, a second group of much larger fragments from a slag pool clustering inside the motor leaves the nozzle.

For the upgraded MASTER-2005 debris model, the SRM dust and slag size distribution parameters have been revised based on newly available impact measurement data. The updated firing database includes 1,076 orbital firings which produce a long-term effect on the debris environment. The processing of all debris generation mechanisms was carried forward up to the reference epoch of May 2005. Due to the deterministic model architecture of MASTER, the flux analysis tool is able to give impact predictions for satellite missions flown in the past considering the orbit propagation of the released particles. The validation of the MASTER-2005 debris population confirmed that the generation model renders good results in terms of flux distribution quality.

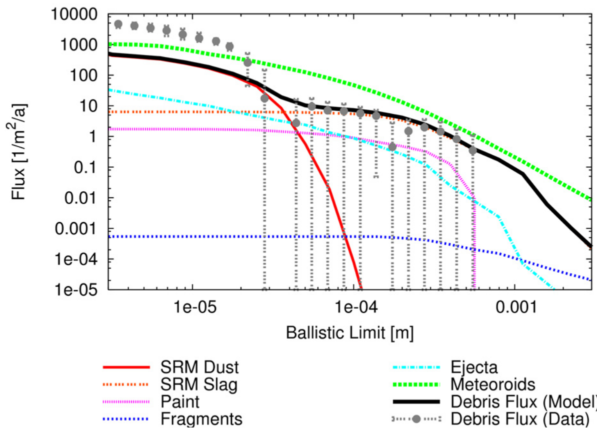

FIG. 1. Flux vs. ballistic limit in aluminium on LDEF's south face, comparison of MASTER-2005 model results with measurement data derived by Unispace Kent [1].

The characteristic shape of the SRM dust size distribution is clearly visible in the cumulative flux distributions. The measured debris flux level for dust can be reproduced with MASTER for satellite surfaces of recent missions such as the solar arrays of the Hubble Space Telescope. The modelled dust flux, however, is under-predicted for some of the analysed LDEF surfaces flown between 1984 and 1990 (compare FIG. 1). This points into the direction of some firings in the past which are not included in the current MASTER-2005 event database. The most suitable candidates for these firings are Russian SRM retro-burns of film return capsules. Under the assumption that Russian retro-engines include the same amount of aluminium in their propellant as other typical SRMs, an analysis was conducted to characterise the influence on the debris environment. The large number of retro-burns

[1] Email address: s.stabroth@tu-bs.de (S. Stabroth)

during the on-orbit time frame of LDEF would be able to form a distinct debris population which could reduce the gap between the modelled and measured historical dust flux for LDEF.

2. RUSSIAN PHOTO RECONNAISSANCE SATELLITES

Since the beginning of spaceflight a large number of Russian photo reconnaissance satellites have been launched. These satellites operate in very low Earth orbits with relatively short mission times in the order of days or weeks. After the mission, the re-entry module containing the film is de-orbited. For this manoeuvre, a retro-burn is required.

The Russian photo reconnaissance satellite program can be divided into different design families: Zenit, Yantar, and Orlets (see FIG. 2). A further classification of the satellite families into different generations was done by Clark [2]. Based on this reference, the satellites of the 3rd generation and possibly those of the 2nd generation use a solid rocket motor for the re-entry manoeuvre.

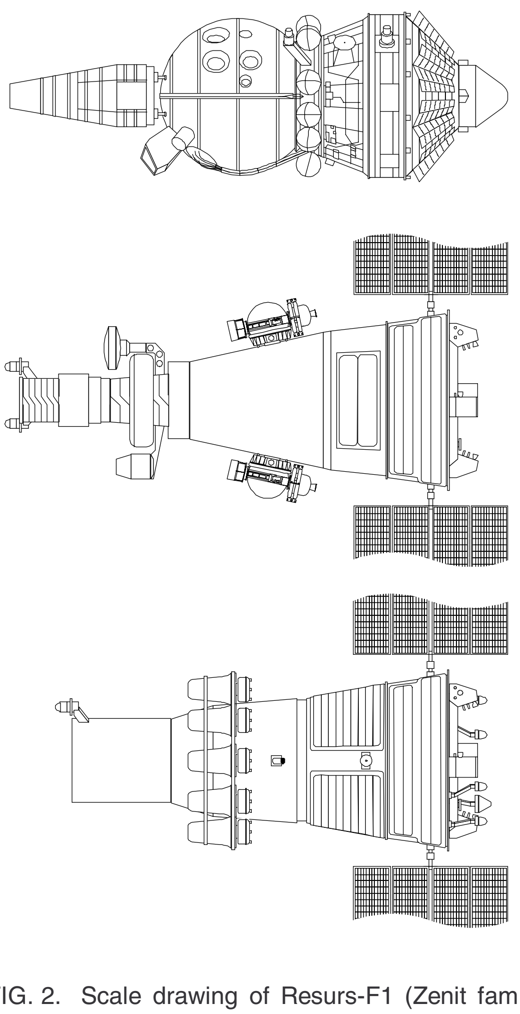

FIG. 2. Scale drawing of Resurs-F1 (Zenit family; top), Yantar (centre), and Orlets-1 (bottom).

For use in civil satellite programs like Resurs-F (remote sensing), Foton (material science), and Bion (biology research), modified Zenit capsules are launched. It is known from a Russian source that Resurs satellites use the TTDU solid rocket motor as the retro-engine [3]. Due to the affiliation to the Zenit family it can be assumed that all Zenit satellites since the 2nd generation and modified satellites thereof use the TTDU retro-engine. The de-orbited mass of each mission is 6,000 kg on average.

The Yantar satellite program consists of a different design. The main re-entry module uses a liquid engine and returns the optics and a subset of the exposed film material back to Earth. In order to increase the orbital lifetime of the Yantar satellites of the 4th generation, two smaller re-entry capsules (designated as SpK – Spuskayemaya Kapsula, descent capsules) are mounted to the landing capsule and camera system module. These capsules use a solid rocket retro-engine (designated as 11D864) for the return of film material to Earth [4],[5]. The engine mass is 52 kg, the overall de-orbited mass of each capsule is unknown to the authors.

The major difference between Yantar and Orlets satellites can be found in the number of small re-entry capsules and the engines used. Orlets satellites of the 6th generation include eight capsules, satellites of the 7th generation contain 22 return capsules. The capsules are arranged in one or two rings around the main satellite body. The retro-engine used by the Orlets capsules is a solid rocket motor designated as 17D712. Since no further information is currently available to the authors, it is assumed that the 17D712 engine provides for the same parameters as the 11D864 engine in terms of overall thrust and propellant mass.

Further satellites like the Arkon program (8th generation) as well as the Zenit 1st generation and Yantar 5th generation satellites are not considered for the purpose of this work since they refrain from using solid rocket motors.

3. SOLID ROCKET MOTOR-FIRINGS

In order to analyse SRM retro-burns and their influence on the debris environment, a literature research on Russian satellite missions with retro-firings was carried out. Up to the end of June 2005, 870 Russian retro-firings with solid rocket motors possibly contributing to the debris environment were identified assuming a successful jettison and re-entry of all capsules. The number of retro-burns with the TTDU motor in the (modified) Zenit program amounts to 508, the number of firings with the 11D864 motor in the Yantar program is 240, and in the Orlets program 122 solid retro-burns took place.

In the next step, a list was compiled including data on the satellite/capsule masses and firing positions (orbits before and after firing). For this purpose, a software program was created which calculates a possible firing location for each re-entry capsule out of Two-Line Elements data sets. The software uses the last known TLE set of a specific satellite [6] and propagates the orbit forward in time under consideration of the J_2 perturbation (rotation of the line of nodes and line of apsides) until the day of re-entry is reached. For the small Yantar and Orlets re-entry capsules, the software assumes the re-entries to be equally distributed throughout the on-orbit mission duration.

The calculation of the firing location depends on the final equator crossing before reaching the landing site of the capsules in Russia. The re-entry trajectory is assumed to proceed from south to north [7]. The landing site is situated between 45.5° to 52° North and 50° to 73.5° East. The software propagates the initial orbits of the capsules and compares the daily equator crossings to the possible final equator crossings leading to an overflight over the landing site on the day of re-entry. If an overflight is possible, the software computes the firing location on the final orbit in a second step where the adjacent re-entry trajectory reaches the landing site. Due to a lack of precise information on the re-entry manoeuvres and object masses involved, the following assumptions had to be applied for the iterative calculation of the firing positions:

- A constant thrust is applied during the burn; 30.7 kN for the TTDU motor [3], and 5.9 kN for the 11D864 motor [5].
- The burn time for the TTDU motor is 23 s [3], and for the 11D864 motor 13 s [5].
- For the small Yantar and Orlets re-entry capsules, a final/initial mass ratio (mass after and before burn) of 0.5 is assumed.
- The SRM fuel mass for the TTDU motor amounts to 246 kg [3]. Using the assumed final/initial mass ratio for the 11D864 motor from above, the fuel mass amounts to 26 kg.
- The 17D712 engine is assumed to have the same parameters as the 11D864 engine in terms of overall thrust and propellant mass.
- The motor exhaust velocity is assumed to be 2.9 km/s which is a typical value for SRMs used in orbit transfers.
- The firing direction for all capsules is assumed to be in the direction of the velocity vector.
- A successful re-entry trajectory is defined by falling short of 50 km altitude above the landing site area.

For 101 of the 870 capsule missions no TLE data sets could be found and the calculation of the firing location with the mentioned software program failed due to an unsuccessful iteration. However, a reasonable firing position could be derived for the remaining 769 firings. FIG. 3 shows the calculated firing altitude of the Zenit, Yantar, and Orlets capsules. The capsules operated in an altitude regime between 150 km and 400 km. An extensive use of the Zenit satellites can be related to the time-frame between 1970 and 1990. The operation of Yantar capsules began in the mid-1970s followed by the Orlets at the end of the 1980s. Since 1995 the number of retro-burns has strongly decreased. The main influence of the Russian retro-burns on the debris environment can therefore be related to the 1980s which is in good accordance with the supposed unmodelled debris flux contribution on LDEF.

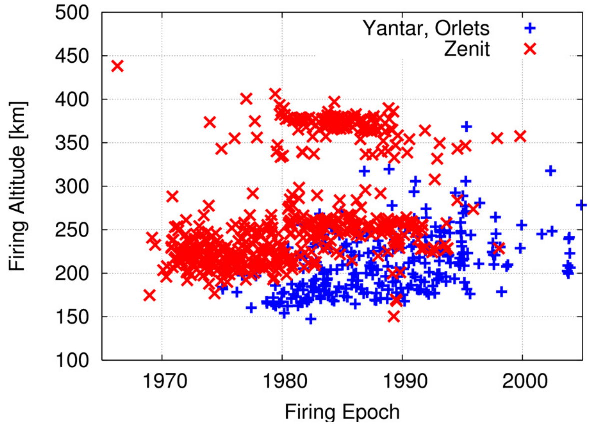

FIG. 3. Computed firing altitude vs. time for all considered Russian SRM retro-burns.

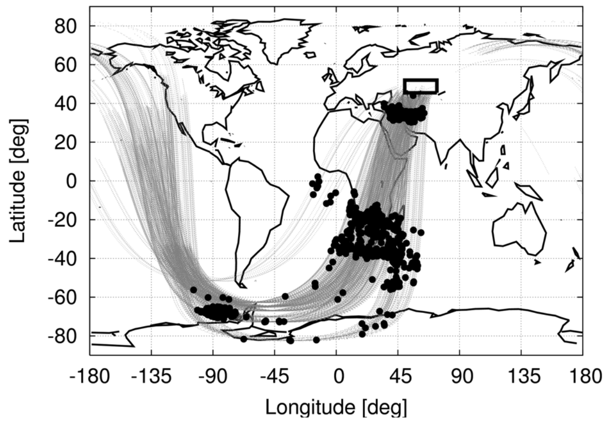

FIG. 4. Computed firing positions and last orbits of Russian film return capsules.

The computed re-entry trajectories strongly differ between Zenit and Yantar/Orlets firings as FIG. 4 shows. Here, half of the orbit before the firing, the re-entry trajectory after the burn, and the firing position itself are plotted for all of the simulated 769 retro-burns. The sub-orbital re-entry orbits of Zenit satellites have small eccentricities (a≈6,400 km, e≈0.03) which result from the low velocity difference (Δv≈0.1 km/s) that the retro-engines can apply due to the large mass to be de-orbited. Therefore, the re-entry firings of those satellites take place in a large distance before the landing site over the south of Africa or the Antarctica, depending on the estimated initial orbit geometry. In contrast, the sub-orbital re-entry flight path of the small Yantar and Orlets capsules sharply declines (a≈4,400 km, e≈0.45). The firing positions are computed to be near the landing site over south-west Asia. This location is the result of the large velocity difference of Δv≈2 km/s that would be achieved for the assumed final/initial re-entry capsule mass ratio of 0.5 and the exhaust velocity of 2.9 km/s. A higher mass ratio and a lower exhaust velocity would result in a smaller Δv and therefore a firing location more to the south. Because no information on the real re-entry flight path is available to the authors, the currently computed firing position has to be seen as a first estimation.

3.1. Simulation of Object Releases

The calculated Russian retro-firing database provides a basis for the calculation of object releases and their influence on the debris environment with the MASTER-2005 software suite. For this purpose, the list of additional firings is handed over to the population generation module POEM (Program for Orbital Debris Environment Modelling). POEM is able to simulate the ejection of SRM particles and their orbit evolution with time [8].

In the frame of this work it is assumed that Zenit, Yantar, and Orlets engines behave comparable to typical orbital SRMs. Orbital SRMs use 18% aluminium powder on average as an additive in the motor propellant mass [8]. During the combustion process, this aluminium chemically reacts with the oxidiser, binding additional oxide molecules to the reaction product. Hence, next to aluminium also part of the oxidiser contributes to the total dust and slag mass generated. Assuming a stoichiometric combustion, this results in a total mass fraction of 34% per firing.

All dust objects generated are assumed to be of spherical shape with an average density of 3.5 g/cm^3. Although in several literature sources a value of 3.97 g/cm^3 is given for the density of aluminium oxide, the parameter as given above has been chosen lower to account for fractions of trapped gas within the particle structure [9].

Each of the computed retro-firings was simulated with the size and ejection velocity distribution model used in the current version of the POEM software [10]. The firings result in particles which are assumed to be ejected into the flight direction. This expels them in particle orbits that are higher than the orbit of the capsule. The very small dust particles have highly eccentric orbits due to the high exhaust velocity. The object perigees reside in the lower regions of the atmosphere while the apogees of the initial orbits can reach geosynchronous altitudes. For slag particles the exhaust velocity is very low and the objects are expelled during the end of the burn only, when the orbit of the capsule is already significantly lowered. This results in near circular orbits for slag objects in the release altitude of TTDU engine firings or in an immediate re-entry of all slag particles for the simulated 11D864 motor firings.

In order to analyse the influence of the released objects on the debris environment each resulting object cloud of the retro-firings was propagated forward in time considering atmospheric drag, solar radiation pressure, major Earth gravitational perturbations, and luni-solar gravity. FIG. 5 and FIG. 6 display the gradual decrease of the share of objects remaining on-orbit after firing. The decrease is not constant with time due to the variable dimension of perturbing effects on the different particle sizes and initial orbit altitudes. It can be shown that the object clouds have orbital lifetimes of up to half a year at maximum, depending on the retro-firing geometry (amount of Δv) and firing altitude. Especially the high apogee of the very small dust particles is lowered in a short time due to the combination of the large area-to-mass ratio and the low perigee of these objects.

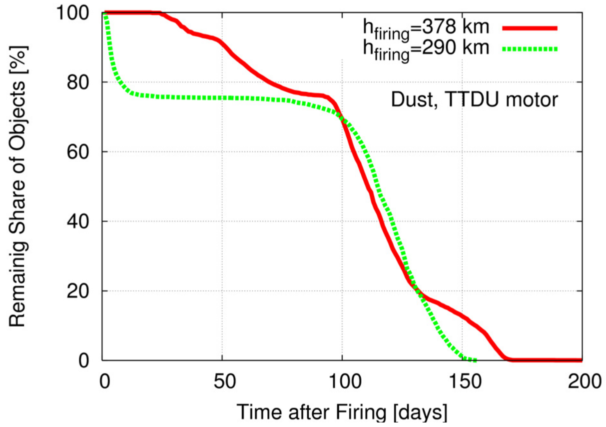

FIG. 5. Evolution of the remaining on-orbit object share for dust particles released by a TTDU engine firing.

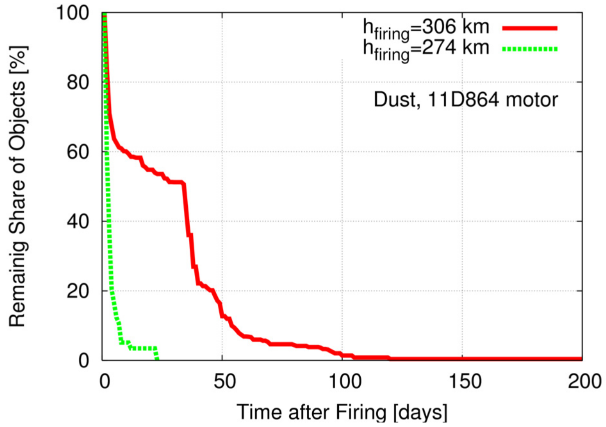

FIG. 6. Evolution of the remaining on-orbit object share for dust particles released by an 11D864 engine firing.

4. INFLUENCE ON THE DEBRIS ENVIRONMENT

From the entire simulation of each computed firing event and the propagation of each object cloud, the influence on the debris environment can be evaluated. FIG. 7 shows the development of the on-orbit mass of the particles released during the simulated retro-firings. The maximum particle mass in orbit amounts to 500 kg during the initial release of objects at specific firings in the early 1980s. The average on-orbit mass in the time frame between 1980 and 1990 is 240 kg. Most of the particle mass in orbit results from firings of the TTDU engine used in the Zenit program as FIG. 7 displays. The contribution of the Yantar and Orlets re-entry capsule firings to the environment is relatively low with an average value of 1 kg on-orbit object mass in the time frame between 1980 and 1990.

The comparison against the already modelled particle population in MASTER-2005 is derived in FIG. 8. Here, the overall on-orbit number of dust objects released by the retro-firings is compared to the background MASTER-2005 SRM dust population. The maximum of the additional objects due to retro-firings is reached in the mid 1980s. Here the high and steady number of events is able to produce a population reaching the order of magnitude of the already modelled dust population of MASTER. Due to the lower number of firings near the end of the 1980s the object number decreases dramatically before 1990.

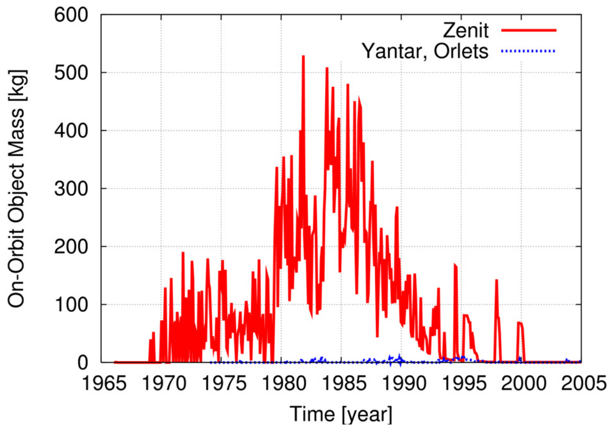

FIG. 7. Evolution of the on-orbit particle mass (released dust and slag objects) of the simulated Russian retro-firings.

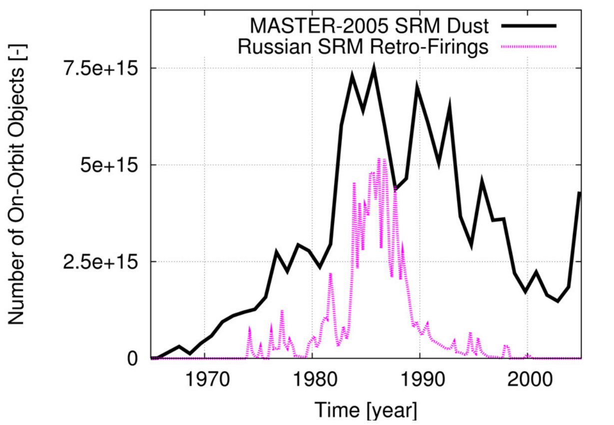

FIG. 8. Evolution of the on-orbit number of objects in comparison with the MASTER SRM dust population.

In comparison to the MASTER-2005 model, the spatial distribution for the 1985 average shows a higher density of the additional dust particles for the Low Earth Orbit regime up to 2,000 km altitude, see FIG. 9. The 1990 density average resides one order of magnitude below the 1985 distribution as expected. In terms of debris flux the largest impact of the Russian retro-firings would therefore be estimated in the year 1985 and 1986 during the on-orbit time frame of the LDEF satellite.

Since the exact impact geometry has to be taken into account for a particle flux analysis on different satellite surfaces, the orbital distribution of the resulting dust population is considered in the following. The particles reside in highly eccentric orbits. The very small objects with high area-to-mass ratios are subject to large orbital perturbations. The initial released particle clouds are constantly removed from orbit by atmospheric drag.

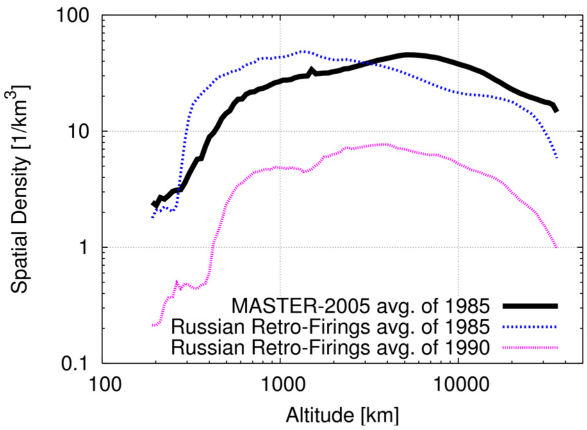

FIG. 9. Comparison of yearly averaged spatial density vs. altitude distributions against MASTER model output.

FIG. 10 shows the spatial density of the retro-firing population (averaged over the on-orbit time frame of LDEF from April 1984 to January 1990) against the altitude and declination angle measured with reference to the Earth equator. The density maximum is reached in the Low Earth Orbit regime at southern latitudes between 60° and 80°. This is the result of the firings simulated to take place in low altitudes in the southern hemisphere placing the perigee of the initial particle clouds at such latitudes.

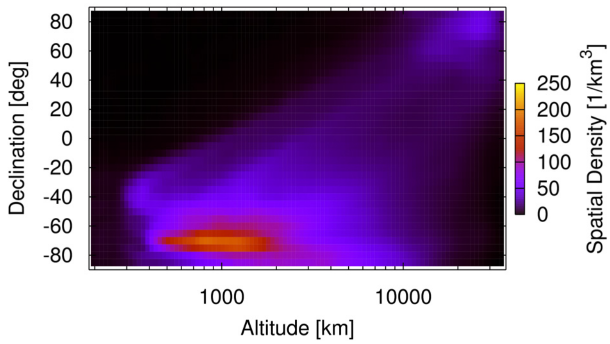

FIG. 10. Spatial density of the retro-firing dust population vs. altitude and declination (averaged over LDEF on-orbit time frame).

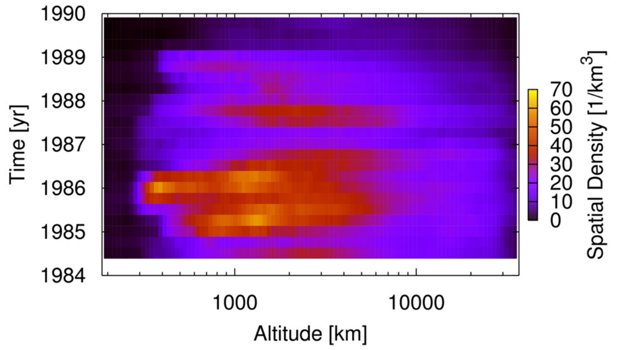

FIG. 11. Spatial density of the retro-firing dust population vs. altitude for the on-orbit time frame of LDEF.

The evolution of the spatial density against altitude during the on-orbit time frame of LDEF is given in FIG. 11. The largest impact of the Russian retro-burns on the LEO debris environment can be seen in 1985 and 1986. Due to the strong decrease in the on-orbit object number since then, it can be concluded that after reaching the high point in 1985/86 the Russian retro-burns pose no ongoing long-term impact on the debris environment.

4.1. Derivation of Impact Flux

The current MASTER-2005 model version considers all known space debris sources such as fragmentations, solid rocket motor firing remnants, NaK droplet releases, paint flakes, and ejecta particles. In terms of firing remnants, the model is based on the simulation of 1,076 historical orbital SRM burns as of May 1st, 2005. The considered firings contribute to the long-term debris environment while firings generating particles with very short orbital lifetimes in the order of hours to some days are neglected. A comparison of the modelled flux with impact data from returned surfaces shows that the shape and quantity of the modelled SRM particle distribution matches that of the recent Hubble Space Telescope (HST) solar array measurements very well [10],[11]. However, the absolute flux level for dust is under-predicted by MASTER-2005 for some analysed Long Duration Exposure Facility (LDEF) surfaces [10], which was the motivation for the work presented in this paper.

In order to compare the influence of the additional firings to the already modelled SRM background flux, the simulation files derived by POEM had to be transformed into database files readable by the MASTER flux analysis tool. The database files consist of probability tables describing the orbital distribution of the dust particles at quarterly snapshot epochs. The probability tables include the cross-coupling between the population distribution parameters namely particle diameter, perigee radius, eccentricity, inclination, and argument of perigee. The particles' right ascension of ascending node is assumed to be equally distributed in the parameter space which accounts for a spreading of the initial clouds with time. The MASTER flux browser reads the probability tables, generates 'on-line' particles and analyses their pass through the Earth's volume discretisation grid. If the particles interfere with the target, the flux contribution of the passes is evaluated. The total resulting flux is cumulated until a pre-calculated reference spatial density is reached. Based on this method, the impact flux on LDEF derived from the retro-firings can be calculated.

Additionally, the derivation of flux distributions vs. impact feature size instead of particle diameter is required for the comparison against measurement data. The flux calculation tool of MASTER-2005 was chosen for this purpose since it allows for a comparison of the modelled vs. measured flux at the common base of the ballistic limit. The ballistic limit represents the maximum foil thickness that can be perforated by a projectile. The transformation from particle diameter to ballistic limit is done in MASTER-2005 with an implemented damage law [12].

4.2. LDEF Flux Analysis

In the following, the contribution of the simulated Russian retro-firings to the absolute flux level on LDEF is analysed. The additional spatial density of the retro-firings at begin of the LDEF mission is calculated higher than the background population of the MASTER-2005 model, compare FIG. 9. Therefore, a higher modelled flux can be expected which should be more in line with the measured LDEF debris flux. However, the exact impact geometry has to be taken into account when analysing the particle flux to the different LDEF surfaces. The high-resolution MASTER-2005 flux browser allows for this analysis.

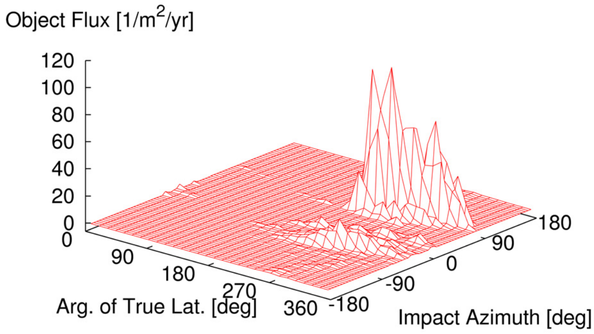

FIG. 12. Distribution of the retro-firing object flux vs. impact azimuth against argument of true latitude of LDEF's orbit (averaged over LDEF on-orbit time frame).

FIG. 12 shows the differential object flux versus impact azimuth and argument of true latitude averaged over the LDEF on-orbit time frame. It is shown that impacts of the additional dust particles on LDEF should have occured at arguments of true latitude between 180° and 360°. The impacts in southern latitudes are due to the distinct argument of perigee distribution of the generated particles in the southern hemisphere (compare FIG. 10) which leads to a conjunction between the particles and LDEF at southern declinations. A large share of the generated particles coincides with LDEF from local south rather than local north directions. This turns into a characteristic flux distribution versus impact azimuth having a large peak between +45° and +90°, see FIG. 13. The impact azimuth is counted positive from the projected velocity vector around LDEF's nadir direction. Because of LDEF's gravity-gradient stabilized flight direction, most of the particles therefore should have impacted the surfaces pointed to the local south direction.

The impact flux direction from the retro-firings is additionally compared with the modelled SRM dust flux in MASTER-2005 in FIG. 13. The shape of the MASTER-2005 flux distribution between ±90° impact azimuth is symmetrical leading to an equal flux contribution to the local north and south surface of LDEF. However, when considering the additional retro-firings the distribution changes and details an asymmetrical contribution with an emphasis between +45° to +90° impact azimuth. Furthermore, MASTER-2005 under-predicts the flux approaching from these azimuth directions. If one considers the estimations given in this paper to be close to reality, it can be concluded that the simulated retro-firings must have been able to account for a large number of debris impacts of very small particles on the southern LDEF surfaces.

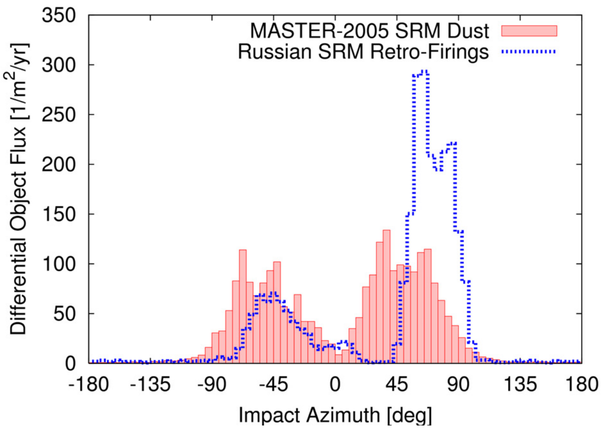

FIG. 13. Comparison of object flux against impact azimuth for MASTER-2005 and the additional firings (averaged over LDEF on-orbit time frame; azimuth counted positive from projected velocity vector around LDEF nadir direction; azimuth class width: 5°).

This result is underlined by comparing the modelled versus measured impact flux for the LDEF surface facing to the local south direction, see FIG. 14. Here, the total debris flux modelled in MASTER-2005 is displayed together with its SRM dust flux contribution and the additional flux derived from the Russian retro-firings. The flux curve is compared to the measured debris flux on the surface [1]. The under-prediction of the MASTER-2005 model is visible for the ballistic limit regime below 30 µm. The debris particle flux in this regime is dominated by dust as the two curves for the MASTER-2005 total debris and SRM dust flux overlap. The MASTER-2005 flux without the additional firings resides one order of magnitude below the measurements at maximum.

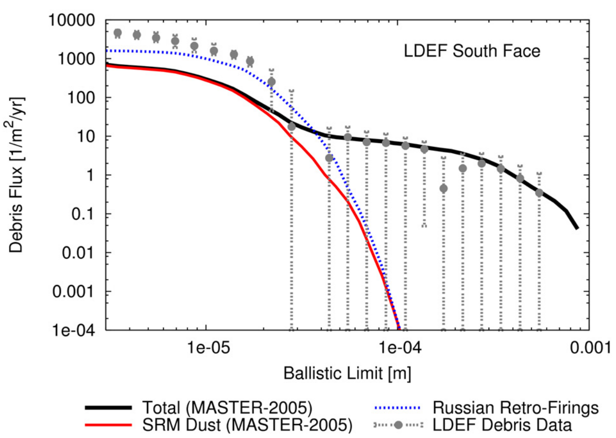

FIG. 14. Comparison of measured and predicted cumulative debris flux vs. ballistic limit for LDEF local south face (debris flux data from Unispace Kent [1]).

It can now be shown that the Russian retro-firings heavily contribute to the overall SRM dust flux environment. The flux distribution on LDEF's south face provoked by the retro-firings exceeds the MASTER-2005 flux level and approaches the measurement points at the 10 µm ballistic limit regime. This flux analysis therefore concludes the consideration of the Russian retro-firings as necessary in order to minimise the historical difference between the measurements and the debris model in the on-orbit time frame of the LDEF satellite. However, it has to be pointed out again that due to the strong decrease in the number of retro-firings since then no ongoing long-term impact on the debris environment is expected.

5. SUMMARY

Solid rocket motors are used in the Russian photo reconnaissance satellite program to return re-entry modules and film capsules back to Earth. In this paper the historical influence of these retro-firings to the debris environment is analysed. A literature research is performed and event lists are compiled. The release of particles during the combustion process of such firings is simulated. The firings are believed to result in the ejection of particle remnants orbiting the Earth in highly eccentric orbits for some days to months before re-entering the atmosphere.

The Russian retro-firings are not considered in the currently available MASTER-2005 model due to having no long-term impact on the debris environment. However, when comparing the model against the measured impact flux for the LDEF mission between 1984 and 1990, the absolute flux level for dust is under-predicted by MASTER-2005. It is shown with this work that the consideration of the large number of retro-firings as a contributor to the overall debris flux minimizes the known differences for the LDEF on-orbit time frame.

However, deviations still exist when comparing historical flux predictions under consideration of the retro-firings with measurements. These deviations can be related to the focus of the presented work which is on the long-term influence of the retro-firings on the environment. The orbital distribution of the resulting dust population is handled the same way as for the creation of MASTER-2005 database files, i.e. providing quarterly snapshot epochs. Due to the discrete character of SRM firings as a debris source, the orbital distribution on a certain snapshot might not implicitly be representative on each considered time span. Instead, the cloud dynamics of the re-entry firings would have to be considered on the short-term (e.g. flux rates on a daily basis) when calculating the cumulative impact flux. A continuation of the work presented here would be highly desirable in this context.

In addition, the work would have to be refined once some of the assumptions made in the paper are replaced by affirmed data. Especially interesting is any further information on the retro-engines, the chemical composition of the propellant, and the re-entry trajectories. Furthermore, currently not considered additional retro-firings of U.S. film return capsules should be analysed in order to extend the database and to calculate their historical influence on the debris environment.

REFERENCES

[1] Anon., Unispace Kent, Meteoroid and Debris Flux and Ejecta Models, Final Report of ESA Contract No. 11887/96/NL/JG, ESA, 1999.

[2] Clark, P.S., Classes of Soviet/Russian Photoreconnaissance Satellite, Journal of the British Interplanetary Society, Vol. 54, pp. 344-360, Hastings, 2001.

[3] Kozlov, D.I. et al., Konstruirovanie Avtomaticheskikh Kosmicheskikh Apparatov, Mashnostroenie, Moscow, pp. 418-435, 1996. (In Russian).

[4] Sorokin, V., Yantarnaya Istoriya, Novosti Kosmonavtiki, Issue 17, page 57, 1997. (In Russian).

[5] Wade, M., Encyclopedia Astronautica, http://www.astronatix.com, last access March 2006.

[6] Anon., Space Track, The Source for Space Surveillance Data, http://www.space-track.org, last access March 2006.

[7] Clark, P.S., Final Equator Crossings and Landing Sites of CIS Satellites, Journal of the British Interplanetary Society, Vol. 54, pp. 21-34, Hastings, 2002.

[8] Wegener, P., Krag H., Rex D., Bendisch J., Klinkrad H., The Orbital Distribution and Dynamics of Solid Rocket Motor Particle Clouds for an Implementation into the MASTER Debris Model, Adv. Space Res., Vol. 23, No. 1, pp. 161-164, 1999.

[9] Hörz, F., Bernhard R.P., See T.H., Kessler D.J., Metallic and Oxidized Aluminum Debris Impacting the Trailing Face of the Long Duration Exposure Facility (LDEF), Space Debris, Vol. 2, No. 1, 2000, pp. 51-66, ISSN 1388–3828, Kluwer Academic Publishers, Dordrecht, The Netherlands, 2002.

[10] Oswald, M., Stabroth, S., Wegener, P., Wiedemann, C., Martin C., Klinkrad, H., Upgrade of the MASTER Model, Final Report of ESA contract 18014/03/D/HK(SC), Institute of Aerospace Systems, pp. 54-90, April 2006.

[11] Anon., Unispace Kent, Post-Flight Impact Analysis of HST Solar Arrays – 2002 Retrieval, Final Report of ESA Contract No. 16283/NL/LvH, ESA, 2005.

[12] McDonnell, J.A.M., Sullivan K., Hypervelocity Impacts on Space Detectors: Decoding the Projectile Parameters, 'Hypervelocity Impacts in Space', J.A.M McDonnell (ed.), pp. 39-47, University of Kent at Canterbury, 1992.